CHIN. PHYS. LETT. Vol. 26, No. 2 (2009) 027301

Influence of Oxygen Vacancy on Transport Property in Perovskite Oxide Heterostructures *

HAN Peng(韩鹏)[1,2], JIN Kui-Juan(金奎娟)[1**], LÜ Hui-Bin(吕惠宾)[1], JIA Jin-Feng(贾金锋)[2] ,
QIU Jie (仇杰)[1], HU Chun-Lian(胡春莲)[1], YANG Guo-Zhen(杨国桢)[1]
[1] *Beijing National Laboratory for Condensed Matter Physics, Institute of Physics, Chinese Academy of Sciences, Beijing 100190*
[2] *Department of Physics, Tsinghua University, Beijing 100084*

(Received 22 October 2008)

Effect of oxygen vacancy on transport property of perovskite microstructures is studied theoretically. Compared with calculated and measured I–V *curves, it is revealed that electron conduction plays an important role in the oxygen nonstoichiometry perovskite heterostructures even with hole-doped or un-doped material due to the oxygen vacancies. In addition, a detailed understanding of the influence of oxygen vacancy concentration and temperature on the conduction characteristics of oxide heterojunction with both forward and reverse biases is obtained by calculation.*

PACS: 73. 40. Lq, 73. 20. Hb, 73. 50. Gr

Perovskite oxide microstructures, including all-oxide or oxide–silicon p–n junction,[1−3], tunnel junction[4], and multilayer structures[5], have attracted great attention since last decade due to their novel properties such as ferromagnetism, ferroelectricity, and photoelectricity. Besides the vigorous research efforts from the experimental aspect, the transport mechanism of the perovskite heterojunction also has been studied from theoretical aspect. Based on the drift-diffusion formulas, Poisson equation, the continuity equations for current, and the interband tunnelling model, the transport processes in the all-oxide[6,7] and oxide-silicon p–n junction[8] have been well explained with both forward and reverse bias,[7] respectively. As indicated in the experimental work,[9] the oxygen contents in perovskite films and junctions are reduced during the fabrication and annealed processes, and this leads to the formation of oxygen vacancies. Moreover, it has been shown that the oxygen content plays an important role on the photovoltaic effect, magnetic property, and transport process in the oxide heterostructures.[10] Although the theoretical[6−8] researches have been carried out in the perovskite oxide microstructures, the effects of oxygen vacancies on the transport processes in these structures are still unclear. Thus, the study of the influence of oxygen vacancy on the transport process in perovskite microstructures is fundamentally important.

Recently, an *ab initio* calculation result revealed that the oxygen vacancy can induce energy states in the forbidden gap of manganite compounds.[11] Furthermore, we have reported that these vacancy induced states can act as trap centres in the trap assisted tunnelling process in p-$La_{0.9}Sr_{0.1}MnO_3$/n-$SrNb_{0.01}Ti_{0.99}O_3$ junction.[7] Besides inducing trap centre states, the shallow energy levels induced by the oxygen deficiency can be taken as a reduction of the band gap in the oxygen nonstoichiometry perovskite material.[11−14] In addition, the oxygen vacancies exhibit the donor character in this kind of materials.[15] Thus, the concentration of electrons in the conduction band of the oxygen nonstoichiometry perovskite is much greater than that in the oxygen stoichiometry perovskite oxide. These electrons not only lead the un-doped insulated perovskite oxide to an n-type semiconductor, but also act as transport electrons in the hole-doped perovskite oxide such as $La_{1-x}Sr_xCoO_{3-\delta}$.[16] However, a theoretical proof is still lacking and few systematic studies have been carried out on the effects of electrons induced by vacancies on the transport process of the perovskite oxide microstructures.

In order to understand the influence of oxygen vacancies on the transport properties in the oxygen nonstoichiometry perovskite microstructures, in this Letter we present the transport processes in such structures with taking into account the electrons induced by the vacancies by solving Poisson equation and the drift-diffusion formulation self-consistently. Our results demonstrate that the electrons induced by oxygen vacancies play an important role in the transport process of the oxide heterostructures with oxygen deficiency. Furthermore, our results also indicate that the uncertainty of the doping type (p-doped or n-doped) we often observed in Hall measurement for hole-doped oxide material may come from the competition of carriers between holes and electrons induced by oxygen vacancies. To verify this mechanism, we present our calculation on the oxygen nonstoichiometry perovskite structures

---

*Supported by the National Natural Science Foundation of China, and the National Basic Research Programme of China under Grant No 2007CB307005.

**To whom correspondence should be addressed. Email: kjjin@aphy.iphy.ac.cn

of $SrTi_{0.8}In_{0.2}O_{3-\delta}/SrNb_{0.01}Ti_{0.99}O_3$ (SITO/SNTO) and $La_{0.7}Sr_{0.3}MnO_{3-\delta}/Si$ (LSMO/Si). The good agreement between the calculated and the measured I–V characteristics reveals that the transport of electrons induced by oxygen vacancies under reverse bias is the physical origin of the leakage current in these systems. In addition, to understand the transport properties of the oxide n–n heterojunction, the I–V characteristics of $LaMnO_{3-\delta}/SrTiO_{3-\delta}$(LMO/STO) heterostructure are calculated with various temperatures and concentrations of oxygen vacancies. It is found that the increase of the concentration of oxygen vacancy in LMO side (with low vacancy concentration) of the heterojunction mainly affects the forward I–V characteristics, while the increase of that in the STO side (with high vacancy concentration) mainly affects the reverse current. In addition, it is also found that both forward and reverse currents increase with the increase of temperature in the oxide n–n junction.

According to the electroneutrality condition, the concentration of electrons induced by the oxygen vacancies $N_{\rm O}$ depends on the concentration of oxygen vacancies and on their states of charge,[15]

$$N_{\rm O} = 2[V_{\rm O}^{\bullet\bullet}] + [V_{\rm O}^{\bullet}], \qquad (1)$$

where, $[V_{\rm O}^{\bullet}]$ and $[V_{\rm O}^{\bullet\bullet}]$ denote the concentrations of singly and doubly ionized oxygen vacancies, respectively. Based on the itinerant electron model for oxygen defect in the hole-doped perovskite oxide,[16,17] the electrons induced by oxygen vacancies are distributed in the conduction band. Thus, the hole-doped oxygen nonstoichiometry perovskite material behaves as a compensated semiconductor. With the complete ionization, the charge neutrality condition in the hole-doped perovskite oxide is expressed as

$$\begin{aligned} &N_c \exp\Big(-\frac{E_c - E_f}{k_B T}\Big) + N_a \\ &= N_v \exp\Big(-\frac{E_f - E_v}{k_B T}\Big) + N_{\rm O}, \end{aligned} \qquad (2)$$

where E_f denotes the Fermi energy; E_c and E_v are the bottom of conduction band and the top of valence band, respectively; N_c and N_v represent the effective density of states function in the conduction and valence band, respectively; N_a denotes the concentration of acceptor; K_B is Boltzmann's constant, and T is the temperature.

Besides exhibiting the donor character, the oxygen vacancy also induces many shallow energy levels in the forbidden gap of the perovskite oxide material. Therefore, the band gap decreases in the oxygen nonstoichiometry oxide, and the principle of semiconductor in thermal equilibrium in such material reads

$$n_0 p_0 = N_c N_v \exp\Big(-\frac{E_g - \Delta E}{k_B T}\Big), \qquad (3)$$

where n_0 and p_0 are the concentrations of electrons and holes in the homogeneous region of the oxide semiconductor, respectively; E_g and ΔE denote the band gap of the material without oxygen vacancy and the decrease of band gap due to the oxygen defects,[11,12] respectively.

According to Eqs. (2) and (3), the concentration of electrons in the conduction band increases and that of holes in the valence band decreases with the increase of the density of oxygen vacancies in the hole-doped perovskite material. The electrons generated by the oxygen vacancies play more and more important role in the transport process in the perovskite heterojunction. In the case that $N_{\rm O}$ is much greater than the concentration of thermal equilibrium electron and much less than that of ionized acceptor density N_a, the effect of electrons induced by the oxygen vacancies on the transport current with forward bias can be omitted, and the drift of these electrons plays a major role in the reverse transport process. For the case that $N_{\rm O}$ is much greater than N_a, the electrons induced by vacancies are the dominant carriers for the transport process with both forward and reverse biases, and an artificial hole-doped oxide can behave as an n-type semiconductor. Therefore, the concepts of majority and minority carrier in semiconductor theory should not be completely applied in the hole-doped oxygen nonstoichiometry perovskite materials. And the majority transport mechanism in such material is determined by the competition between the currents carried by electrons and holes.

In the multicorrelated perovskite oxide system we studied, the behaviour of electrostatic potential $\phi(x)$, the electron concentration $n(x)$ and the hole concentration $p(x)$ with external bias voltage $V_{\rm bias}$ are obtained by solving the coupled Poisson equation, drift-diffusion formulation, and current continuity equation self-consistently.[6,7] The detailed arithmetic for solving these equations has been introduced in the previous work.[6,7,18] The electrostatic potentials at the boundary of two sides are set as $\phi(0) = 0$ and $\phi(L) = V_d \pm V_{\rm bias}$, respectively, with V_d denoting the build-in potential. The concentrations of electron and hole far away from the space charge region are set to

$$\begin{aligned} p(0) &= \frac{N_a - N_O}{2} \\ &+ \sqrt{\Big(\frac{N_a - N_O}{2}\Big)^2 + N_c N_v \exp\Big(-\frac{E_g - \Delta E}{k_B T}\Big)}, \\ n(0) &= \Big[N_c N_v \exp\Big(-\frac{E_g - \Delta E}{k_B T}\Big)\Big]/p(0), \\ n(L) &= N_d, \quad p(L) = n_i^2(L)/N_d, \end{aligned}$$

where N_d denotes the ionized donor density, $n_i(L)$ denotes the intrinsic concentration at the n side of the junction.[19]

To verify the mechanism of electron conduction, we present our calculation on the SITO/SNTO homojunction with parameters given in Ref. [6]. The comparison between the experimental (hollow squares) and the theoretical (solid curve) I–V curves with the calculated tunnelling current (dotted curve) is plotted in Fig. 1 at $T = 300\,\mathrm{K}$ with doping density of $N_a = 7.34 \times 10^{18}\,\mathrm{cm}^{-3}$ and $N_d = 1.63 \times 10^{19}\,\mathrm{cm}^{-3}$, respectively.[6] This junction was fabricated under $3 \times 10^{-4}\,\mathrm{Pa}$ oxygen pressure and was annealed for 30 min under the oxygen pressure of about $1 \times 10^{-2}\,\mathrm{Pa}$. The concentration of electrons induced by the oxygen vacancies is chosen as $1.0 \times 10^{18}\,\mathrm{cm}^{-3}$ and ΔE is chosen as 0.4 eV in our calculation.[14] Because the concentration of acceptors is greater than that of electrons induced by vacancies, the behaviour of carriers with forward bias is the same as that in a p–n junction. With reverse bias, the electrons induced by oxygen vacancies in the conduction band of p-SITO drift into the n-region with the increase of reverse bias and form a non-saturation leakage current. In addition, as shown in the inset of Fig. 1, the barrier width between the valence band of p-side and the conduction band of n-side is about 50 nm with $V_{\mathrm{bias}} = -1.5\,\mathrm{V}$, thus the effect of tunnelling can be omitted. Therefore, the drift of electrons induced by the oxygen vacancies is proven to be the physical origin of the leakage current in the SITO/SNTO junction at reverse bias.

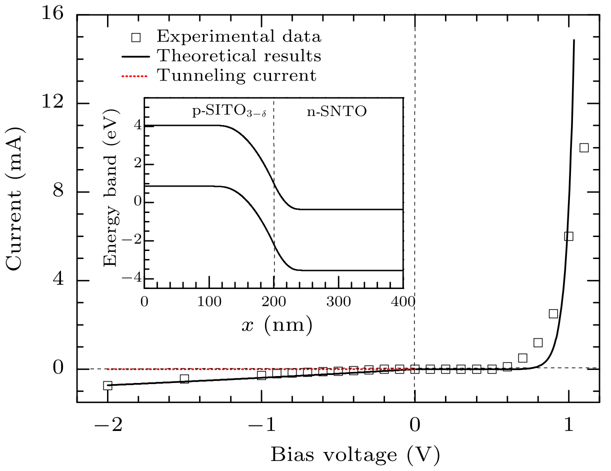

Fig. 1. Theoretical and experimental I–V curves of SITO/SNTO junction with reverse and forward biases at $T = 300\,\mathrm{K}$. The experimental data are obtained from Ref. [6]. Inset: the band structure of LSAO/SNTO junction with $V_{\mathrm{bias}} = -1.5\,\mathrm{V}$.

For further studying the effects of oxygen vacancy on the transport process in oxide heterojunction, we plot the calculated (solid curve) and the measured (hollow squares) I–V curves of LSMO/Si heterojunction with the calculated tunnelling current (dotted curve) at $T = 300\,\mathrm{K}$ in Fig. 2, respectively. The calculated band-energy profile with $-1.5\,\mathrm{V}$ bias is indicated in the inset of Fig. 2. This LSMO layer was fabricated and annealed with the pressure of oxygen of about $3 \times 10^{-2}\,\mathrm{Pa}$. The doping densities N_a and N_d are taken as $1.0 \times 10^{20}\,\mathrm{cm}^{-3}$ and $1.0 \times 10^{16}\,\mathrm{cm}^{-3}$, respectively. The concentration of electrons induced by the oxygen vacancies N_{O} is chosen as $5.0 \times 10^{15}\,\mathrm{cm}^{-3}$, ΔE is chosen as 0.2 eV, and the other necessary parameters are taken from Ref. [8]. It should be pointed out that a series resistance of $3.8\,\mathrm{k\Omega}$ is introduced in calculation to fit the effect of the contact resistance and substrate resistance as we have treated in our previous work.[8] The good agreement between the calculated and measured data gives a further verification that the reverse leakage current originates from the drift of electrons induced by the oxygen vacancies in the hole doped region.

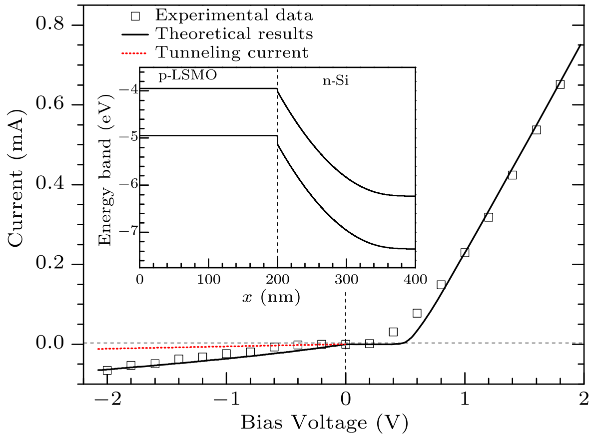

Fig. 2. Theoretical and experimental I–V curves of LSMO/Si junction with reverse and forward bias at $T = 300\,\mathrm{K}$. The experimental data are taken from Ref. [8]. Inset: the band structure of LSMO/Si junction with $V_{\mathrm{bias}} = -1.5\,\mathrm{V}$.

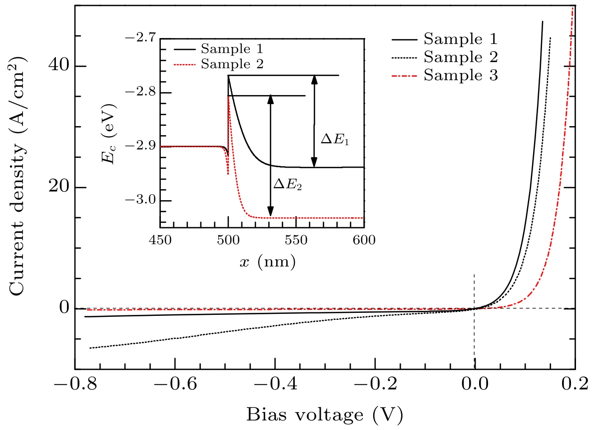

Fig. 3. Calculated I–V curves of LMO/STO n–n junction with various concentrations of oxygen vacancies in sample 1 ($N_{\mathrm{OL}} = 5.0 \times 0^{16}\,\mathrm{cm}^{-3}$ and $N_{\mathrm{OR}} = 5.0 \times 10^{17}\,\mathrm{cm}^{-3}$, solid curve), sample 2 ($N_{\mathrm{OL}} = 1.0 \times 10^{16}\,\mathrm{cm}^{-3}$ and $N_{\mathrm{OR}} = 2.5 \times 10^{18}\,\mathrm{cm}^{-3}$, dotted curve), and sample 3 ($N_{\mathrm{OL}} = 1.0 \times 10^{16}\,\mathrm{cm}^{-3}$ and $N_{\mathrm{OR}} = 5.0 \times 10^{17}\,\mathrm{cm}^{-3}$, dashed curve) at $T = 300\,\mathrm{K}$, respectively. Inset: the bottom of conduction band of sample 1 and 2 with $V_{\mathrm{bias}} = 0.15\,\mathrm{V}$.

Furthermore, to understand the effect of the concentration for the oxygen vacancies on the transport property in oxide heterojunctions, we calculate the I–V curves with various concentrations of the oxygen vacancies N_{OL} in LMO side and N_{OR} in STO side of an LMO/STO n–n junction. Similar to p–n junction, the material with low Fermi level is set as the left side of the n–n junction and the material with high Fermi level is set as the right one, respectively. The calculated I–V curves of sample 1 ($N_{\rm OL} = 5.0 \times 10^{16}\,{\rm cm}^{-3}$ and $N_{\rm OR} = 5.0 \times 10^{17}\,{\rm cm}^{-3}$, solid curve), sample 2 ($N_{\rm OL} = 1.0 \times 10^{16}\,{\rm cm}^{-3}$ and $N_{\rm OR} = 2.5 \times 10^{18}\,{\rm cm}^{-3}$, dotted curve) and sample 3 ($N_{\rm OL} = 1.0 \times 10^{16}\,{\rm cm}^{-3}$ and $N_{\rm OR} = 5.0 \times 10^{17}\,{\rm cm}^{-3}$, dashed curve) are plotted in Fig. 3, respectively. As indicated in this figure, with the increase of either $N_{\rm OL}$ or $N_{\rm OR}$, both forward and reverse currents increase due to the increase of the concentration of electrons induced by the oxygen vacancies. In addition, the effect of $N_{\rm OL}$ on the current density with forward bias is greater than that of $N_{\rm OR}$, while $N_{\rm OR}$ dominates the property of current under reverse bias. To understand the behaviour of current with forward bias, the barrier height of the conduction band with $V_{\rm bias} = 0.15\,{\rm V}$ for sample 1 ($\Delta E_1 = 0.17\,{\rm eV}$) and 2 ($\Delta E_2 = 0.23\,{\rm eV}$) are plotted in the inset of Fig. 3, respectively. Here ΔE_1 and ΔE_2 are determined by the difference between the work function of the two sides of the n–n junction. As shown in this figure, the greater barrier height of sample 2 reduces the Richardson thermal emission current, which dominates the transport property at forward bias. In the case of reverse bias, the electron drift current increases rapidly in sample 2 due to its high build-in potential caused by the great difference between the concentrations of oxygen vacancies in two sides of the junction.

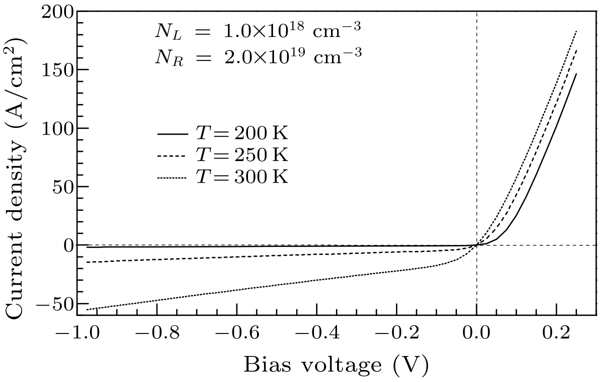

Fig. 4. Calculated I–V curves of LMO/STO n–n junction with various temperatures $T = 200\,{\rm K}$ (solid curve), 250 K (dashed curve), and 300 K (dotted curve), respectively. The concentrations of oxygen vacancies in the left and right side of the junction are $N_{\rm OL} = 1.0 \times 10^{18}\,{\rm cm}^{-3}$ and $N_{\rm OR} = 2.0 \times 10^{19}\,{\rm cm}^{-3}$, respectively.

To reveal the effect of temperature on the I–V characteristics of n–n junction, we plot the I–V curves of the oxygen nonstoichiometry LMO/STO heterojunction with $T = 200\,{\rm K}$ (solid curve), 250 K (dashed curve), and 300 K (dotted curve) in Fig. 4, respectively. The concentrations of the oxygen vacancies for the left and right side of the junction are $N_{\rm OL} = 1.0 \times 10^{18}\,{\rm cm}^{-3}$ and $N_{\rm OR} = 2.0 \times 10^{19}\,{\rm cm}^{-3}$, respectively. As indicated in this figure, both the forward and reverse currents increase with the increase of temperature. This behaviour is attributed to the effect of Richardson thermionic emission current, which governs the transport process across the interface of the heterojunction.

In summary, the transport properties in the oxygen nonstoichiometry perovskite microstructures have been studied theoretically. Our results reveal that the oxygen vacancies play a dominant role on an un-doped oxide thin film, even in p-type oxide film in which not only holes but also electrons contribute to the current. As a result, an artificial hole-doped oxide can behave as a compensated semiconductor and an un-doped oxide can become an n-type semiconductor due to the increase of the concentration of electrons induced by the oxygen vacancies. We believe that the uncertainty of the doping type (p-doped or n-doped) we often observed in the Hall measurement in the hole-doped oxide material may be attributed to the oxygen vacancy. In addition, it is found that the variation of the concentrations of oxygen vacancies in one side of the oxide heterojunction mainly affects the forward or reverse I–V characteristics, respectively. Furthermore, our results reveal that both forward and reverse currents in the oxide n–n junction increase with the increase of temperature. These results not only give a new insight into the microscopic transport property of the perovskite heterostructures but also provide a reliable scheme to estimate the concentration of oxygen vacancies in the oxide heterostructures by measuring the I–V characteristics.

References

[1] Tanaka H et al 2002 *Phys. Rev. Lett.* **88** 027204
Mitra C et al 2003 *Phys. Rev. Lett.* **90** 017202
[2] Lu H B et al 2005 *Appl. Phys. Lett.* **86** 032502
Jin K J et al 2005 *Phys. Rev.* B **71** 184428
[3] Hunter D et al 2006 *Appl. Phys. Lett.* **89** 092102
[4] De Teresa J M et al 1999 *Phys. Rev. Lett.* **82** 4288
O'Donnell J et al 2000 *Appl. Phys. Lett.* **76** 1914
Alldredge L M B et al 2006 *Appl. Phys. Lett.* **89** 182504
[5] Newns D M et al 1998 *Appl. Phys. Lett.* **73** 780
[6] Zhou Q L et al 2005 *Europhys. Lett.* **71** 283
[7] Han P et al 2007 *Appl. Phys. Lett.* **91** 182102
Han P and Jia J F 2008 *Phys. Lett.* A **372** 4943
[8] Qiu J et al 2007 *Europhys. Lett.* **79** 57004
[9] Sun J R et al 2004 *Appl. Phys. Lett.* **84** 4804
Li G et al 2007 *Appl. Phys. Lett.* **91** 163114
[10] Xiong C M et al 2007 *Appl. Phys. Lett.* **91** 053510
[11] Picozzi S et al 2007 *Phys. Rev.* B **75** 094418
[12] Sterne P A and Wang C S 1988 *Phys. Rev.* B **37** 7422
[13] Hossain F M et al 2007 *Solid State Ionics* **178** 319
[14] Selme M O and Pecheur P 1983 *J. Phys.* C **16** 2559
[15] Moos R et al 1995 *Appl. Phys.* A **61** 389
[16] Lankhorst M H R et al 1996 *Phys. Rev. Lett.* **77** 2989
[17] Sogaard M et al 2006 *Solid State Ionics* **177** 3285
[18] Horio K et al 1990 *IEEE Trans. Electron. Devices* **37** 1093
Han P et al 2006 *J. Appl. Phys.* **99** 074504
[19] Neamen D A 2003 *Semiconductor Physics and Devices Basic Principles* 3rd edn (New York: McGraw-Hill)